

Techno-environmental and economic assessment of off-grid hybrid energy systems for combined cooling, heating, power, and battery-hydrogen storage

Mohamad Reza Mehdizadeh Marzebali^a, Masoumeh Mohamadian^{a,*}

^a Department of Energy Engineering and Physics, Amirkabir University of Technology (Tehran Polytechnic), P.O. Box 15875-4413, Tehran, Iran.

Keywords

Off-Grid Hybrid Energy Systems
Multi-Storage Systems
Design Builder
HOMER
CCHP systems

Article Info

DOI: [10.22060/AEST.2025.5749](https://doi.org/10.22060/AEST.2025.5749)

Received 20 Jan 2025

Accepted 22 Feb 2025

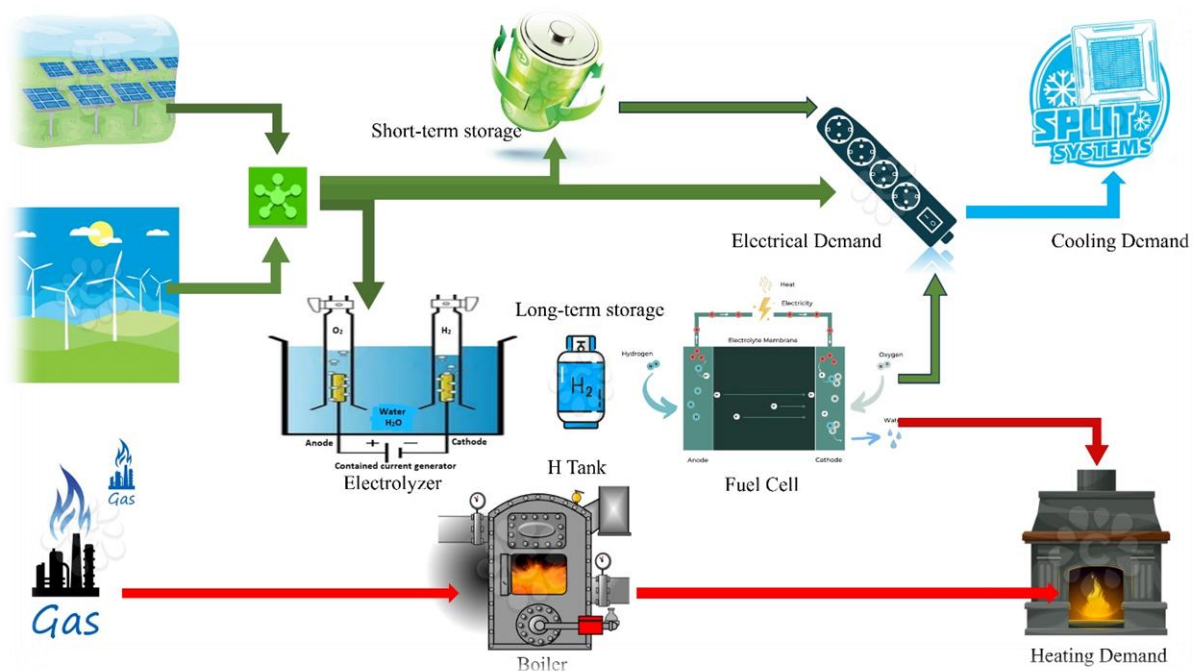
Published 1 June 2025

Corresponding author:
Mohamadian@aut.ac.ir

Abstract

This study addresses the urgent energy challenges associated with climate change, exacerbated by industrialization and rapid population growth, through the simulation of a renewable energy system at Amirkabir University. Using Design Builder, we assessed the energy demands for electricity, cooling, and heating in a faculty building, and subsequently developed a combined generation and multi-storage system in HOMER that integrates renewable energy sources, natural gas, and advanced storage solutions, including hydrogen and batteries. Our analysis compares the performance of systems utilizing 1 kW and 10 kW wind turbines, demonstrating that the 10 kW turbine significantly outperforms its smaller counterpart. Solar energy contributes 1,931,801 kWh (89%) to the system, while wind energy accounts for 216,261 kWh (10%). The economic evaluation reveals a total present cost of \$6.77 million for the system with the 10 kW turbine, yielding a production cost of \$0.377 per kWh and reducing CO₂ emissions to 102,586 kg/year. Furthermore, sensitivity analysis indicates increased wind energy production under higher wind speeds, validating the potential for wind energy in Tehran. Overall, this research highlights the effectiveness of integrated renewable energy systems in mitigating greenhouse gas emissions and meeting rising energy demands over a projected 20-year lifespan while demonstrating significant economic viability.

Graphical Abstract



1. Introduction

Climate change is one of the most pressing global challenges today, driven by factors such as greenhouse gas emissions and the industrial revolution, which have led to increased energy consumption. Researchers are actively seeking solutions, with combined generation and multi-storage systems gaining importance. Multi-energy complementary distributed energy systems (MECDES) integrated with renewable energy sources are at the forefront of sustainable energy development, offering significant potential for energy conservation and emission reduction [1]. As resource shortages become more critical, new energy technologies and sources are receiving widespread attention.

The combined cooling, heating, and power (CCHP) system is an efficient and stable energy utilization method, with promising applications for achieving energy ladder utilization and multi-energy complementarity [2]. The building sector is a major energy consumer, presenting substantial opportunities for reducing energy consumption. Current energy systems in buildings are increasingly incorporating renewable sources such as solar and wind power. However, fully developing a multi-generation energy system reliant solely on these sources is challenging without adequate energy storage, backup systems, or grid connections [3]. Reducing reliance on fossil fuels is essential for lowering greenhouse gas emissions, with renewable energy sources like solar, wind, and geothermal providing viable alternatives [4].

Optimizing the use of wind and photovoltaic (PV) power to decrease dependence on the power grid for integrated energy systems (IES) is a key area of research. Solar energy systems effectively meet the requirements for heating, cooling, electricity, and domestic hot water, but incorporating energy storage units is crucial for achieving sustainability [5]. Various energy storage options include electrical, thermal, hydrogen, carbon dioxide (CO₂), and hydro systems [6]. The future of energy generation is leaning towards green hydrogen, produced from renewable energy sources. Hydrogen serves as a means of storing energy generated from these resources, with electrolyzers facilitating sustainable hydrogen production [7]. Recent studies have proposed innovative CCHP systems integrating molten carbonate fuel cells (MCFC), integrated solar gas-steam combined cycles (ISCC), and double-effect absorption lithium bromide refrigeration (DEALBR) systems. These new CCHP systems demonstrate improved performance, lower CO₂ emissions, and the capability to simultaneously meet cooling, heating, and electricity demands [8]. Reference [9] presents a comprehensive hydrogen utilization system based on a CCHP framework, including hydrogen production processes. An evaluation system encompassing thermal economics, technical economics, and environmental protection factors is established to assess the performance of the comprehensive utilization system. A case study involving an office building analyzes the performance of solid oxide fuel cell (SOFC) and phosphoric acid fuel cell (PAFC)-based systems, comparing technical economic outcomes across different regions [9]. In addition, a comprehensive renewable energy supply system has been developed to tackle the significant energy demand in buildings located in Zhengzhou, China. This system efficiently delivers cooling, heating, and electricity by integrating sustainable energy sources like solar, hydrogen, wind and geothermal energy, while economic and engineering studies enhance their integration [10].

Another study configures a new energy system to address these global challenges by simulating a building as a real case study to extract energy demands. This approach aims to achieve sustainable agriculture through optimization procedures. From an environmental perspective, the implementation of hybrid energy systems can avoid 83% to 100% emissions [11]. A different research study presents an economic, energetic, and environmental consideration of combined cooling, heating, and power systems utilizing solid oxide fuel cell technology (SOFC-CCHP) for a cancer care hospital. A 3D model of the hospital structure was created using eQUEST software to accurately assess the energy requirements of the current system (baseline scenario). The findings reveal that the levelized cost of electricity is \$0.087/kWh for this system, with a payback

period of 10 years based on the designed capacity of the SOFC. Additionally, the SOFC-CCHP system achieves an 89% reduction in CO₂ emissions annually compared to the hospital's existing system.[12]. The conventional CCHP system is capable of supplying cooling, heating, and electricity only. However, study [13] presents a CCHP system that allows for independent regulation of refrigeration and dehumidification using a proton exchange membrane fuel cell (PEMFC). The system model is developed using MATLAB/Simulink. Study [14] shows that under design conditions, the outputs of the power, heating, and cooling outputs of the modified solid oxide fuel cell combined CCHP (MR-SOFC-CCHP) system are 226.9 kW for electricity, 46.6 kW for cooling, and 36.4 kW for heating. The system achieves a thermal efficiency of 81.6% and an energy output efficiency of 59.7% [14].

Paper [15] presents an innovative energy system that combines hydrogen production with its distribution. With the CCHP system and incorporates significant wind power to address these dual challenges. This new system has the potential to lower costs and carbon dioxide emissions, conserve primary energy, and significantly enhance energy efficiency [15]. Study [16] presents a transient performance and techno-economic assessment of an innovative smart energy system utilizing a combination of solar and hydrogen energy. This system is intended to fulfill the electricity, heating, and cooling requirements of a two-story structure. It consists of fuel cells, photovoltaic thermal panels, a small-scale Organic Rankine Cycle, a solar collector, and thermal energy storage units. The system is analyzed from technical, economic, and environmental perspectives, employing a tree-objective optimization method to find the optimal solution across all mentioned indexes [16]. Study [17] proposes an integrated energy system that effectively utilizes extra photovoltaic power to generate hydrogen. This system integrates hydrogen production, solar energy, and the CCHP system to generate heating, cooling, power, and also hydrogen. It provides energy to three public facilities achieving the minimum unit energy cost of \$0.0615 per kWh achieved through optimization. Two comparative approaches were employed to assess the integrated power system based on unit energy cost, total annual costs, fossil fuel consumption, and carbon dioxide emissions. Following this, analyses of the total annual energy, standard daily energy demands, and costs of the system were conducted and optimized [17].

Following the mathematical modeling of the components, the system components are optimally sized using HOMER Pro software. An evaluation of techno-economic-environmental is conducted to analyze fossil fuel reduction, green hydrogen production through electrolyzers, and storage via hydrogen tanks and fuel cell systems. A literature review comparing articles utilizing HOMER software is presented at Table 1 [18]. The aforementioned reasons underscore the necessity for a comprehensive technical, economic, and environmental analysis to address energy challenges and the crises that arise from them. Consequently, analyzing hybrid energy systems for the utilization of renewable sources is essential for reducing dependence on fossil fuels and the conventional grid, alongside implementing suitable storage solutions. As a result, an off-grid hybrid system has been designed that integrates both green hydrogen production and effective storage options. While previous research has acknowledged the significance of battery storage systems, a notable gap was identified in the literature concerning hydrogen storage systems. This gap presents an opportunity to enhance energy storage capacity and system reliability by integrating hydrogen storage with batteries.

Table 3. Overview of Related Literature on Similar Studies Conducted in Other Locations.

Country	Hybrid Design	NPC, \$	COE, \$/kWh	Year	Daily Electricity Consumption, (kWh/day)	Peak Load, kW	Reference
Kenya	PV/Diesel/Battery, off-grid	7,568,600.45	0.354	2017	2944	360	[19]
Spain/Madrid	PV/Battery	1,490,589	€0.25-0.4	2018	634	350-550	[20]
Turkey/Istanbul	PV/Wind/FC/H2	8,724,232	3.391	2011	627		[21]
	Wind/FC/H2	9,900,033	3.847	2011			[21]
Saudi Arabia, Yanbu	PV/Wind/Battery, off-grid	1,434,950	0.617	2017	556	68	[22]
Malaysia	PV/DG/Battery/converter	1,500,000-2,450,000	0.151-0.233	2018	2138.50	213.60	[23]
Cameroon	PV/Diesel/small hydro/battery	0.443		2019	100	35.18	[24]
India	PV/FC/Battery + H2	47,437	0.203	2017	56.52		[25]
Patani	PV-wind turbine-pumped hydro storage		0.27	2020			[26]
Nigeria	Solar/Micro-Hydro/Diesel/Battery	963,431	0.112	2020	3375	357	[27]
Cameroon	Photovoltaic/Wind/Biogas/Pumped Hydro	370,426	€0.256	2018	348.02	57.88	[28]

In this study, solar and wind energy are considered for Tehran without interference from the grid. Given that wind speeds in Tehran are relatively low, it is possible that the system may not be technically or economically feasible. Therefore, this research aims to assess the system's viability by comparing two turbine capacities: 1 kW and 10 kW, selecting the one with higher efficiency for further analysis. If the system proves infeasible, an increase of an additional two meters per second will be applied to the wind speed to evaluate at which speed this system could become viable in a city with characteristics similar to Tehran. This innovative approach not only addresses existing gaps in hybrid energy systems but also contributes to the development of sustainable energy solutions tailored to specific urban environments. By integrating hydrogen storage with conventional battery systems, this research aims to enhance overall energy reliability and efficiency while promoting the use of renewable resources in urban settings. The study will include a roadmap outlining the following:

1. Site identification
2. Design of the integrated energy system
3. Analysis of solar, wind, and temperature resources
4. Components of the integrated system
5. Mathematical models for various components and financial metrics
6. Load profile of the case study.

1.1. Site description (Case Study)

The location for this analysis is situated within one of the departments of Amirkabir University of Technology in Tehran, Iran. The department is situated at coordinates 35°43.3' N and 51°20.1' E, according to data from NASA. The surrounding community primarily consists of students. The building has a total floor area of 11,000 m² and consists of 9 floors, each

with a height of 4.55 m. Below is a summary of the climatic conditions of the studied area. The average temperature is 11.67 °C, and the average wind speed is 3.39 m/s, also based on data from NASA.

1.2. Design Builder

To simulate the building's energy consumption and determine its load demands, we utilized DesignBuilder software. Initially, we gathered essential data about the building, including architectural plans, materials, and weather conditions such as solar radiation and hourly temperature. This information was then inputted into DesignBuilder to generate a 3D model of the structure.

1.3. Solar and Wind Energy Resource

For the simulation, we used mean monthly data on global horizontal solar radiation and the clearness index for the site, covering a 22-year period from 1983 to 2005, as documented by NASA. Fig. 1-Fig. 3 is illustrated this data. The research area enjoys robust solar radiation year-round, with average annual solar radiation of 4.89 kWh/m² per day. The maximum solar radiation levels are observed in June, while due to the rainy season December experiences the lowest. The clearness index for Tehran is maximum in September, averaging 0.646, and lowest in December, with a mean of 0.523. This suggests that a substantial quantity of solar radiation reaches the Earth's in the study place.



Fig. 1. Clearness index and monthly mean solar radiation for our case study.

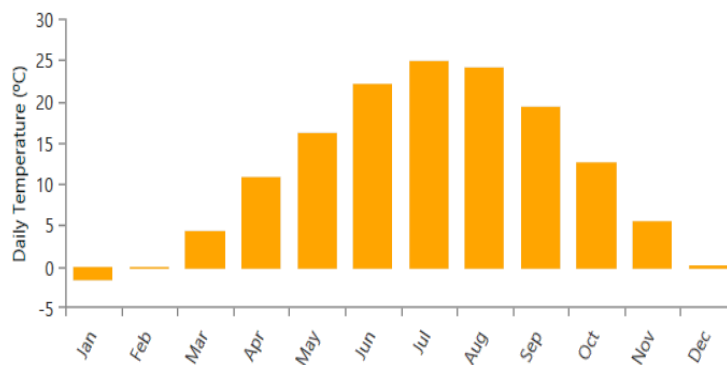


Fig. 2. Monthly average temperature data for Tehran.

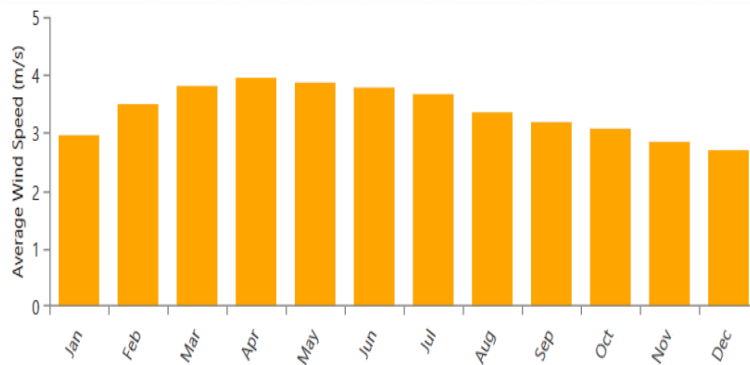


Fig. 3. Monthly average wind speed for the case study.

The proposed system incorporates both conventional and renewable resources, a combination that enhances reliability, lowers overall costs, and facilitates more effective optimization.

5. Methodology

2.1. Hybrid Renewable Energy System (HRES) Modeling and Operation

This hybrid renewable energy system is designed to efficiently integrate various energy sources and storage mechanisms to address diverse energy demands, including electricity, heating, and cooling. By combining renewable sources such as solar and wind with traditional fossil fuels like natural gas, the system ensures a reliable and sustainable energy supply.

The system harnesses solar energy through solar panels and captures wind energy using wind turbines. The electricity generated from these renewable sources is managed via a combination of short-term and long-term storage solutions. Short-term storage is facilitated by batteries, specifically a 1 kW lead-acid battery, which stores excess electricity for immediate or near-term use.

For long-term storage, the system employs a power-to-power (P2P) mechanism that utilizes an electrolyzer to convert surplus electricity into hydrogen gas (H_2) through electrolysis. This hydrogen is subsequently stored in an H_2 tank. When electricity is needed, the stored hydrogen is fed into a fuel cell, which converts the hydrogen back into electricity to meet electrical demand.

Additionally, the system incorporates an electric chiller to satisfy cooling requirements by utilizing the generated electricity. Natural gas is deployed to fulfill heating demands through a boiler and heating system [19]. Also, depicts the overall configuration of the hybrid renewable energy system, illustrating how the different components interact to provide a stable and flexible energy supply.

2.2. Case Study Database

For this study, various types of input data were collected. The site description includes geographic coordinates and the building's address. Building details encompass the floor area, number of floors, user type, and building height. Climate and weather condition data include temperature, solar radiation, wind speed, and seasonal variations. Technical data consist of specifications for the system components, while economic data involve the inflation rate, interest rate, and associated costs. Project data includes the expected lifetime of the projects (Table 2).

Table 4. Data requirements for this study.

Kind of input Data	Description of the Input Data
Site Description	Geographic coordinates such as longitude, latitude, and address of the site building
Building Details	Detailed Plan of the building, Floor Area, number of floors, building user type, height of building and floors, schedule time
Climate & weather conditions	Meteorological data such as Temperature, solar radiation and clearness index, wind speed data and its seasonal variation
Technical data	Technical data of the components
Economic data	Inflation rate, interest rate, economic data of the components
Project data	Life time of the projects

2.3. Mathematical Modeling of System Components

It should be noted that the operational strategy of the system adheres to the following electrical load (FEL).

In this section, the methodology of the research is detailed, covering the description of various systems and equipment used in renewable energy production and storage. The primary aim is to provide technical details and relevant equations for the functioning of different energy systems, including photovoltaic panels, wind turbines, converters, battery storage systems (BSS), electrolyzers, fuel cells (FC), and hydrogen tanks. Each section thoroughly describes the operation and mathematical formulas related to these processes to enhance understanding of the involved energy production and management methods.

2.3.1 PV

Flat photovoltaic panels convert solar radiation into electrical power, with their output influenced by the characteristics of the PV technology and the temperature of the cells. The PV power equation is presented at Eq. (1) [20]:

$$P_{PV} = P_{PV \text{ rated}} * f_{dPV} * G/1000 * [1 + \alpha(T_{cell} - 25)] \quad (2)$$

Where, $P_{PV \text{ rated}}$ demonstrates the rated power of the photovoltaic panel, f_{dPV} is the derating factor for the panel (3% per year), G represents solar radiation (W/m^2), the temperature coefficient of power is α ($0.49\%/^{\circ}C$), and the cell temperature is T_{cell} . Additionally, the total efficiency of the module is considered to be 15.3%

2.3.2 Wind Turbine

The output power of wind turbines varies between different models, depending on the turbine's power curve and the wind characteristics of the deployment site. The hourly power output of a wind turbine at a specific location is influenced by factors such as air density, rotor area, power coefficient of the turbine, and the hourly wind velocity V (m/s). The equation Eq. (2) and Fig. 4 illustrate how the turbine's output power is affected by its power curve [21]:

$$P_{WT} = \begin{cases} 0 & V \leq V_{cuttin} \\ \frac{P_{rated}}{V_{rated}^3 - V_{cuttin}^3} V^3 - \frac{V_{cuttin}^3}{V_{rated}^3 - V_{cuttin}^3} P_{rated} & V_{cuttin} \leq V \leq V_{rated} \\ P_{rated} & V_{rated} \leq V \leq V_{cutoff} \\ 0 & V > V_{cutoff} \end{cases} \quad (2)$$

As shown in Fig. 5, V_{cut-in} represents the cut-in wind speed (m/s), $V_{cut-off}$ denotes the cut-off wind speed (m/s), and V_{rated} is the wind speed (m/s) at which the turbine generates its rated power (P_{rated}) [19]. The power curves for this analysis are based on a generic 1kW and 10 kW wind turbine model. This research employs two models of wind turbines, one kilowatt and ten kilowatts, from the brand Excel-S. The study aims to compare the energy production of the one-kilowatt turbines with that of the ten-kilowatt turbines to determine which model yields a higher output. Overall, the results will be analyzed to evaluate the efficiency and effectiveness of each turbine size in energy generation.

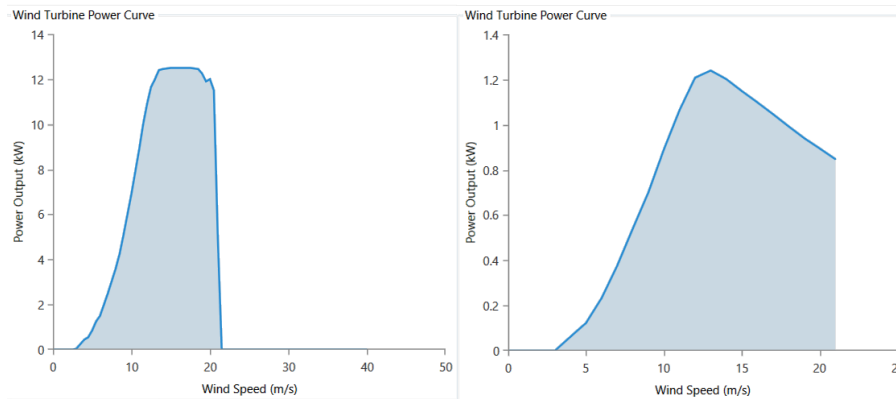


Fig. 4. Power curves of the 10 kW and 1 kW Bergy Excel wind turbine.

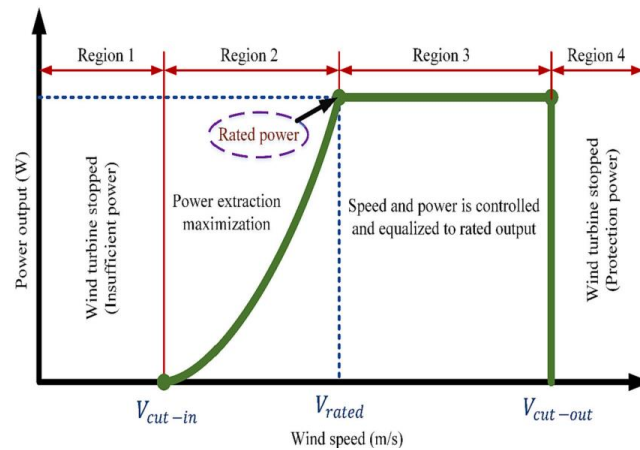


Fig. 5. Wind turbine characteristics.

2.3.3 Converter

Transfer of energy across the AC bus and the DC bus is facilitated using a converter. This converter is a three-phase dual mode hybrid type, bi-directional, specifically designed for mini-grid systems. Produced by Leonics in Bangkok, it has a lifespan of ten years. In this research, an inverter model with an efficiency of 92 % is evaluated, and the output power of inverter is expressed by the following Eq. (3) [22-23]:

$$P_{inv,out} = (P_{PV} + P_{batt} + P_{storage}) * \eta_{inv} \tag{3}$$

2.3.4 Battery Storage System (BSS)

It is mainly incorporated into renewable energy generation systems to help maintain stable and consistent operations, particularly by regulating voltage levels when there is a discrepancy between power consumption and generation. To achieve increased energy capacity and reliability, it is advisable to connect batteries with identical rates both in parallel and

in series [24]. It is crucial to determine the ampere-hour (A.h) and watt-hour (W.h) capacities of the BSS to adequately meet load demands over extended periods. This consideration is essential for managing fluctuations in energy production from renewable sources, such as wind and solar energy [24]. The W.h capacity of the battery can be determined by the following Eq. (4) [25]:

$$C_{wh} = \frac{(E_L \times AD)}{(\eta_{bat} \times \eta_{inv} \times DoD)} \quad (4)$$

Where AD represent the daily autonomy of the battery; E_L (kWh/day) represents the mean daily load energy, DoD indicate the battery depth of discharge, and the efficiencies of the inverter and battery are represented by η_{inv} and η_{bat} , respectively. For the analysis, the battery from surrette company was utilized, with a maximum capacity of 1,890 Ah, a 4V nominal voltage, a rate constant of 0.528 per hour, a nominal capacity of 7.55 kWh, a capacity ratio of 0.254, a maximum 459A charge current and a round-trip efficiency of 80%.

2.3.5 Electrolyzer

Because of its efficiency in high energy, electrolysis is a well-established and effective method for hydrogen production. This process is particularly well-suited for incorporation with renewable energy generation systems, such as those utilizing solar and wind power [26]. Electrolyzers typically generate hydrogen only when operating beyond a minimum threshold, typically established between 25% and 40% of the units' nominal production capacity [27]; this study adopts a threshold of 25%. This operational limit is crucial for preventing the formation of potentially flammable hydrogen and oxygen mixtures. As previously mentioned, the hydrogen system serves as a storage solution. In this context, both charging and discharging processes can be employed and are represented as follows [28] which using the electrolyzer in charging mode (Eq. 5):

$$E_{st}(t) = E_{st}(t - 1) + \left(E_{pv}(t) - \frac{E_L(t)}{\eta_{inv}} \right) \eta_{Ele} \quad (5)$$

Where $E_{st}(t - 1)$ and $E_{st}(t)$ represent the energy stored in the hydrogen storage tanks in two consecutive times. Additionally, $E_L(t)$ demonstrates the energy demand, and $E_{pv}(t)$ represents the energy produced by the photovoltaic panels. η_{Ele} , η_{inv} are the efficiencies of the electrolyzer and the inverter, respectively.

2.3.6 Fuel Cell

It is an electrochemical tool that transforms chemical energy into electrical energy, functioning similarly to a battery. The key distinction between fuel cells and conventional batteries is that while batteries are energy accumulators with their maximum output limited by the amount of stored chemical reagents, fuel cells can continuously produce electricity as long as they are supplied with fuel, limited only by the degradation or malfunction of their components.

In hydrogen fuel cells, hydrogen serves as the reducing agent at the anode, while oxygen acts as the oxidizing agent at the cathode. In fact, a fuel cell is made up of a stable catalytic electrode, in which the positive electrode (cathode) interacts with the oxidant, while the negative electrode (anode) interacts with the reductant. These electrodes are separated by a membrane or electrolyte. The chemical reactions in a fuel cell produce heat, electricity, and water, which promotes its advancement as an energy conversion system that is both clean and sustainable.

A fuel cell operates fundamentally in the opposite manner to hydrolysis: hydrogen undergoes oxidation at the anode, while oxygen is reduced at the cathode, resulting in a difference in potential between the two electrodes. The voltage difference can be captured via another circuit, provided that an insulating electrolyte is inserted between the cathode and anode, which

allows only ions to pass through, thereby facilitating transfer of charge [29]. Using the fuel cell operating in discharge mode by Eq. (6) [28]:

$$E_{st}(t) = E_{st}(t - 1) - \frac{E_L(t) - E_{pv}(t)}{\eta_{FC}} \quad (6)$$

Where $E_{st}(t - 1)$ and $E_{st}(t)$ represent the energy held in the hydrogen storage tanks. Also, $E_L(t)$ demonstrate the energy demand, and $E_{pv}(t)$ represents the energy generated by the PV collectors. η_{FC} is the fuel cell efficiency.

2.3.7 Hydrogen Tank

The hydrogen generated through green methods is kept in a hydrogen tank for future use as needed. In this study, the stored hydrogen is allocated for the creation of low-carbon ammonia intended for fertilizer manufacturing, considering there is an available resource of nitrogen. Further details on this application are discussed in the following.

The estimated costs associated with the hydrogen tank include an initial capital cost of \$1.5/kg, a replacement cost of \$0.5/kg, and annual operation and maintenance (O&M) expenses of \$0.6 [30]. The hydrogen tank and electrolyzer were measured concurrently, ranging from 50 to 1000 kW and 2000 to 10,000 kg, respectively. The ideal configurations are those combinations of hydrogen tank and electrolyzer that yield the minimum levelized cost of hydrogen. The mass of hydrogen can be quantified as an electrical energy function stored in the tank (Eq. (7)) [31]:

$$M_{tank}(t) = \frac{E_{tank}(t)}{HHV_{H_2}} \quad (7)$$

Where HHV_{H_2} refers to the higher heating value of hydrogen gas, which is commonly estimated to be 39.7 kWh/m² and $E_{tank}(t)$ is expressed as Eq. (8) [32]:

$$E_{tank}(t) = E_{tank}(t - 1) + \left(P_{Elect-tank}(t) - \frac{P_{tank-FC}(t)}{\eta_{storage}} \right) \times \Delta t \quad (8)$$

Where $E_{tank}(t-1)$ denotes the electrical energy stored in the hydrogen gas tank during the previous interval, $P_{tank-FC}$ represents the power flow from the hydrogen tank to the fuel cell (FC), $\eta_{storage}$ is the efficiency of the hydrogen gas tank, which is 95% and Δt is the time interval between simulated values.

6. Optimization and Objective Functions

3.1. Renewable Fraction

The renewable fraction refers to the portion of energy delivered to the load that comes from renewable sources. It is calculated using the equation Eq. (9) [33]:

$$f_{ren} = 1 - \frac{E_{non\ ren} + H_{non\ ren}}{E_{served} + H_{served}} \quad (9)$$

Where $E_{non\ ren}$ denotes non-renewable electrical production [kWh/yr], $H_{non\ ren}$ represents non-renewable thermal production [kWh/yr], E_{served} is the total electrical load served [kWh/yr], and H_{served} refers to the total thermal load served [kWh/yr].

3.2. Environmental Assessment

As previously stated earlier, one of the primary factors in the deployment of hybrid energy systems (HES) is the reduction of emissions in greenhouse gas (GHG). This research as an environmental consideration evaluates direct CO₂ emissions in

the development of HES components. In the suggested HES, CO₂ emissions arise from three resources: (i) electricity generation by the micro gas turbine (MGT) generator; (ii) thermal energy production with the gas boiler; and (iii) the procurement of grid electricity. The total annual emissions of this GHG are calculated using the following Eq. (10) [34]:

$$CE = CE_{MGT}m_{MGT} + CE_{boiler}m_{boiler} + CE_{grid} \times E_{grid} \quad (10)$$

Where m_{MGT} , m_{boiler} , CE_{MGT} and CE_{boiler} represent the overall quantity of natural gas used by the boiler and MGT, along with their corresponding emission coefficients. CE_{grid} represents the average factor of emission for electricity production in power plants, while E_{grid} indicates the net power acquired from the grid—calculated as the difference between sold and electricity acquired—over a year for HES operation. Since we do not have access to the grid or MGT, only emissions from the boiler are operation.

3.3. Economic Evaluation

The analysis will focus on both economic factors and annual environmental CO₂ emissions (tons/year). The economic criteria will be divided into three sub-criteria: Net Present Cost (NPC) in dollars, Levelized Cost of Electricity (LCOE) in (\$/kWh), and annual operating cost (\$/year) [35].

NPC is a key economic indicator in project evaluation. It encompasses the present value of all expenses throughout the project's lifespan, including capital costs, fuel costs, replacement costs, operation and maintenance (O&M) costs, emissions penalties, and the costs associated with purchasing power from the grid. The NPC is calculated by deducting the present value of all system revenues—such as salvage value and revenue from grid sales—from the total costs. This is achieved by aggregating the total discounted cash flows for each year of the project's duration. The Capital Recovery Factor (CRF) is utilized to determine the present value of the project's cash flows over its lifetime and is calculated using Eq. (11) [35].

$$CRF(r, L) = \frac{r(1+r)^L}{(1+r)^L - 1} \quad (11)$$

Where L represents the lifetime of the project and r denotes the real discount rate, calculated as follows Eq. (12) [35]:

$$r = \frac{IN - IF}{1 + IF} \quad (12)$$

Where IN and IF represent the annual interest rate and inflation rates (%), respectively. The Levelized Cost of Electricity (LCOE) is described as the average cost per kilowatt-hour (kWh) of useful electrical energy produced by the system, and it can be determined using the following Eq. (13) [35].

$$LCOE = \frac{C_{ann,tot} - C_{boiler} H_{served}}{E_{served}} \quad (13)$$

Where $C_{ann,tot}$ is the total annualized cost of the system (\$/year), C_{boiler} represents the marginal cost of the boiler (\$/kWh) and H_{served} and E_{served} denote the total thermal and electrical loads served (kWh/year), respectively. In this context, $C_{ann,tot}$ is calculated as Eq. (14) [35]:

$$C_{ann,tot} = CRF(r, L) \cdot C_{NPC} \quad (14)$$

Annual operating cost is another critical economic factor to be determined, calculated using Eq. 15 [35]:

$$C_{o\&m} = C_{ann,tot} - C_{ann,cap} \quad (15)$$

Where $C_{ann,cap}$ is the total annualized capital cost (\$/year). According to the rates published by the Central Bank of Iran, the discount rate is established at 18%, while the annual inflation rate is set at 16% for the project's 20-years duration [36].

3.4. Homer Pro software

The Hybrid Optimization Model for Electric Renewables (HOMER Pro) software, created by the NREL, which is designed to model, design, and optimization of various hybrid energy systems. HOMER serves as a valuable tool for analyzing hybrid renewable microgrid systems, integrating elements such as wind turbines, fuel cells, biomass, hydropower, converters, PV systems, batteries, traditional generators, and combined heat and power (CHP) systems.

Table 3 [37] presents the advantages and disadvantages of HOMER software, while Table 4 [18, 36, 38, 39, 40, 41] provides cost information for the components used within the software.

Table 3. Advantage and Disadvantage of HOMER.

Advantages	Disadvantages
Providing a list of real technologies simulated based on available equipment.	Being time-consuming and slow for some solutions.
Quite accurate simulation results for analysis and evaluation.	Requiring for accurate input data.
Providing a list of possible configurations based on different technologies and different equipment sizes.	Requiring experience-based criteria to achieve a good solution.
Solving many configurations quickly.	High quality of input data (resources).
Utility of results in learning to optimize systems with different combinations.	Software's inability to guess key values or sizes in case of their absence.

Table 4. Cost of Components.

Equipment	COST (\$/kw)		O & M (\$/Year)
	Capital Cost	Replacement	
Photo Voltaic	1000	750	55
Wind Turbine- Excel- S	1650	1650	10
Fuel Cell- CHP	400	400	0.01
H Tank	1.5	0.5	0.6
Electrolyzer	100	100	5.00
Battery Storage	150	100	10
Converter	400	300	10

7. Results

4.1. Building simulation design

After creating the 3D model of the building, it will be displayed as Fig. 6. Once the simulation is complete, the load demands are extracted and input into HOMER software. Fig. 7 shows the final demand loads of the building that were entered into HOMER.

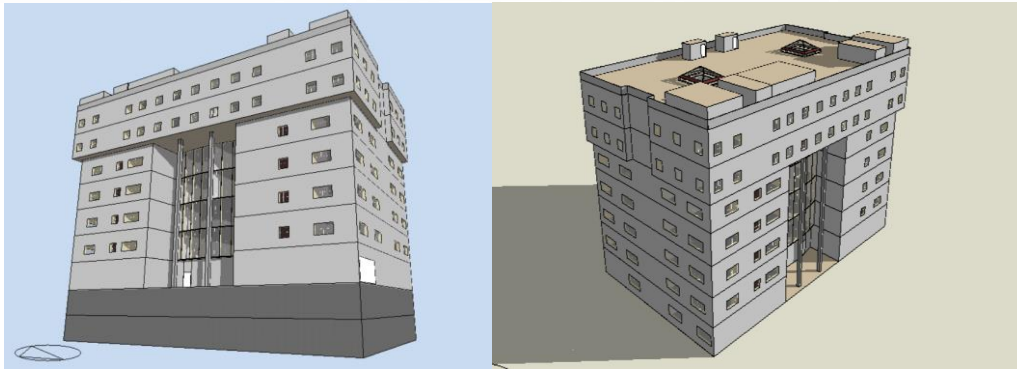


Fig. 6. Case Study Department in Design Builder.

Electricity demand primarily comes from lighting, laboratory devices such as ovens, centrifuges, and computers, as well as projectors and other equipment frequently used in the department. This demand remains constant throughout the year and does not vary with the seasons. Cooling needs arise from electrical chillers used to cool classrooms; during winter and autumn, there is no demand, resulting in a blacked-out heat map. Heating demand is driven by the need for domestic hot water and space heating in the department, peaking during the winter months.

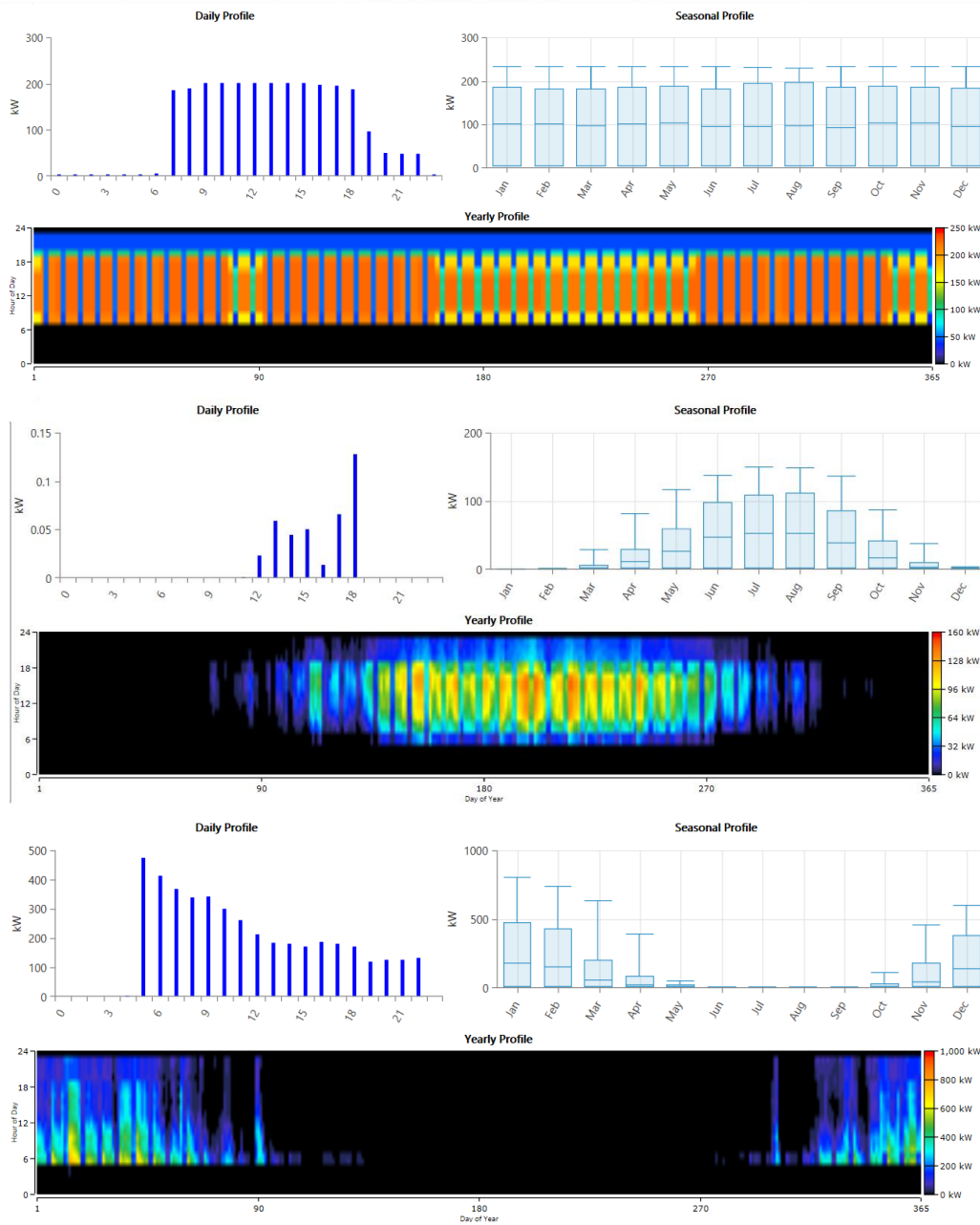


Fig. 7. The first, second and third figures are: load, cooling and heating load.

4.2. Configuration design

After designing the system as outlined in the configuration section, the first figure in HOMER displays the energy supply schematic. Fig. 8 shows the configuration of the designed system.

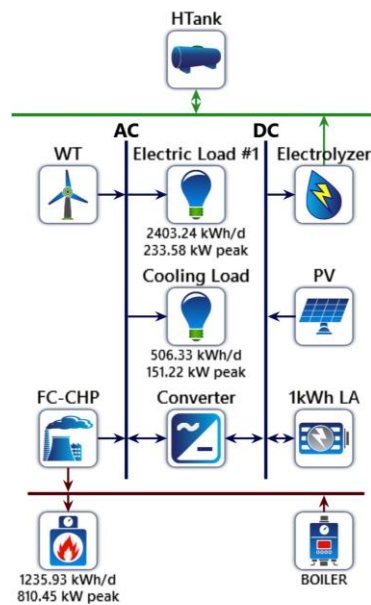


Fig. 8. Schematic of the system design energy supplier.

4.3. Total Production and Cost

In this section, the contribution of each component of the system to electricity production is presented in a Table 5. The total capacity of the wind turbines was evaluated by selecting between one-kilowatt and ten-kilowatt models, assuming that the unit cost of capacity is the same for both. The system employs a singular turbine size exclusively for the entire wind power component, without mixing different sizes. This approach is based on the assumption that the unit cost of capacity is equivalent for both models. The results indicate that if one-kilowatt turbines are selected, the system optimally allocates approximately 95% of electricity production to photovoltaic panels, while wind energy accounts for roughly 5%. Conversely, if ten-kilowatt turbines are chosen, the share of wind energy increases to 10%, with photovoltaic panels contributing about 89%.

Additionally, the production of hydrogen electricity from fuel cells has significantly increased, making hydrogen storage a more viable option. According to Table 5, the reduction in photovoltaic panel capacity from 2,042,853 kW to 1,931,801 kW, coupled with the increase in wind energy efficiency share from 112,852 kW to 216,261 kW, will lead to a reduced disparity in efficiency between the renewable energy sources.

Table 5. The contribution of each component to total electricity production.

Component	Production - kW	
	Selecting Wind Turbine 1 kW	Selecting Wind Turbine 10kW
PV	2042853	1931801
Fuel Cell	51628	18988
WT	112852	216261
Total	2160873	2167051

Consequently, selecting ten-kilowatt turbines has proven to generate greater overall production for the system at a lower cost while also improving wind energy efficiency in Tehran, which is not ideally suited for wind energy due to its lower wind speeds. Therefore, as the system evaluation continues, ten-kilowatt turbines will be selected.

4.4. Economical evaluation

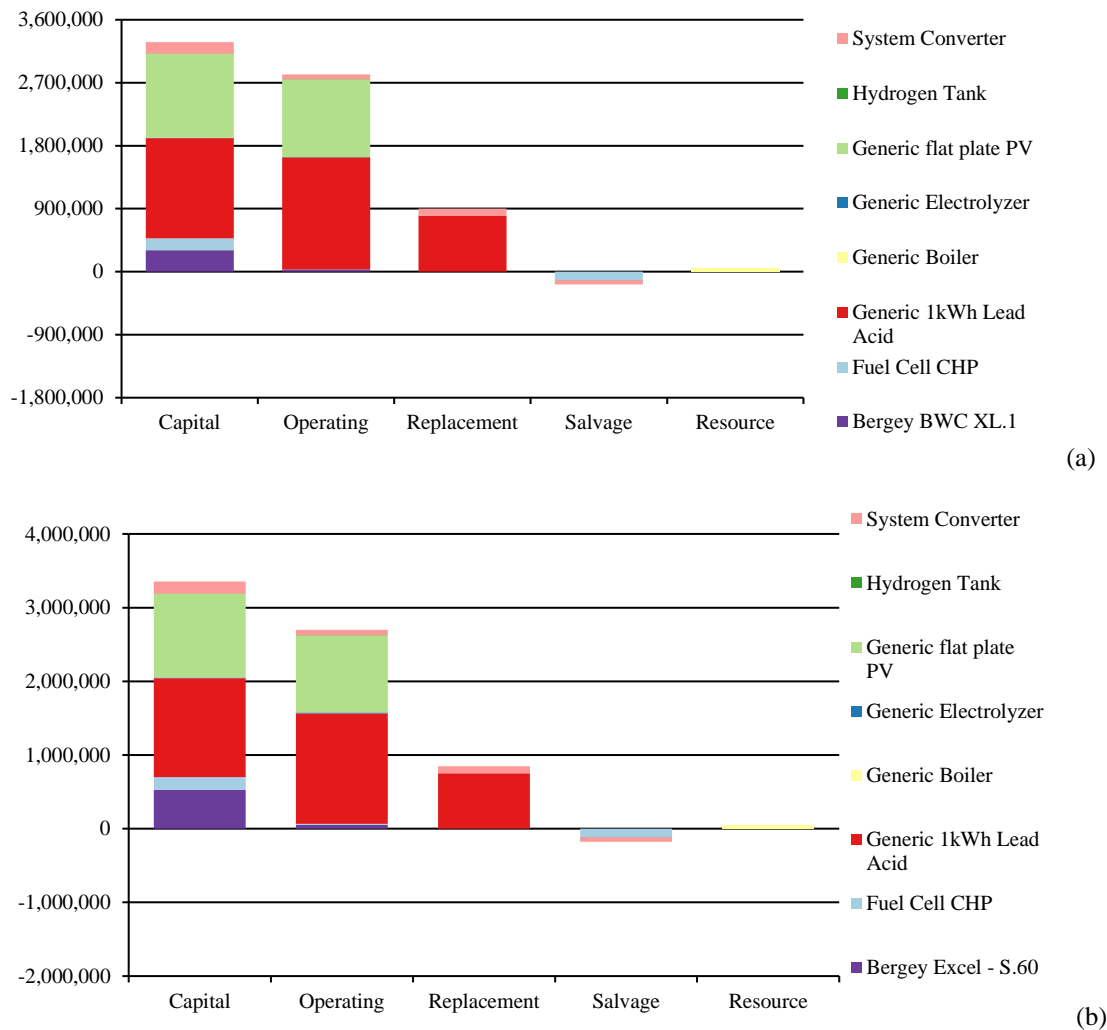


Fig. 9. Net present cost of each equipment. (a) 1 kW. (b) 10 kW.

This section provides a comprehensive overview of the capital, replacement, operational, disposal, and fuel consumption costs associated with systems featuring 1 kW turbines (Fig. 9-a) and 10 kW turbines (Fig. 9-b). The majority of costs are attributed to the battery segment, totaling \$3.84 million for the 1 kW turbine system and \$3.59 million for the 10 kW turbine system. Given that the system operates off-grid and relies on intermittent renewable energy sources, storage systems are essential for capturing excess energy during periods of high production for use during peak demand.

Following battery costs, photovoltaic panels represent a significant expense, with total costs of \$2.31 million for the 1 kW turbine system and \$2.19 million for the 10 kW turbine system. Due to the shorter lifespan of batteries and converters compared to the overall project duration, replacement costs will be incurred throughout the project. In contrast, both the photovoltaic panels and wind turbines have lifespans that align with that of the project, thereby avoiding disposal costs. The data also indicates negative disposal costs, suggesting that these costs are effectively returned to the project as income rather than representing an expense.

In terms of current total costs, the implementation of 1 kW turbines incurs an expense of \$6.87 million, resulting in an electricity cost of \$0.383 per kWh. Conversely, a system utilizing 10 kW turbines has a total current cost of \$6.77 million

and a lower electricity production cost of \$0.377 per kWh. This indicates that the selection of 10 kW turbines yields greater overall production at a lower cost, while also enhancing wind energy efficiency in Tehran, which is not ideally suited for high wind speeds. Opting for this configuration facilitates a more cost-effective utilization of the larger capacity provided by wind turbines. Consequently, as the system evaluation progresses, the selection of 10 kW turbines will be prioritized.

4.5. Fuel and Emission evaluation

The only fossil fuel used in this system is natural gas, which the boiler utilizes for the system's thermal load. Meanwhile, the fuel cell features a heat recovery system and operates as a combined heat and power (CHP) unit, generating both power and heat, with hydrogen stored as fuel. The only component that produces CO₂ emissions is the boiler.

In the system utilizing 1 kW turbines, a total of 1,574 kg of hydrogen fuel is consumed, whereas the system with 10 kW turbines consumes 5,707 kg of hydrogen fuel. This difference indicates that the hydrogen storage system in the 10 kW turbine setup is more efficient. Furthermore, the increased hydrogen fuel consumption in the fuel cell generates additional heat, which supports the boiler and contributes to a reduction in natural gas consumption.

The fuel consumption for the boiler in the 1 kW turbine system is 53,498 cubic meters, while the system with 10 kW turbines shows a lower consumption of 52,935 cubic meters. This reduction in fuel usage ultimately leads to decreased environmental emissions. Table 6 illustrates the total emissions for both systems.

Table 6. Emissions of the system.

Pollutant	Quantity		Unit
	System with 1 kW turbine	System with 10 kW turbine	
Carbon Dioxide	103,787	102,586	kg/yr
Carbon Monoxide	26.0	94.2	kg/yr
Unburned			
Hydrocarbons	1.13	4.11	kg/yr
Particulate Matter	0.157	0.571	kg/yr
Sulfur Dioxide	0	0	kg/yr
Nitrogen Oxides	24.4	88.5	kg/yr

4.6. Optimal Sizing

4.6.1 Finding the suitable Turbine

Based on the previous findings, the selection of 10 kW turbines has optimized the system's energy production while reducing overall costs from an economic standpoint. Furthermore, this choice has led to a decrease in emissions, enhancing the system's environmental sustainability. Consequently, subsequent analyses will concentrate on the capacity details and components of the system featuring the 10 kW turbines.

Table 7 indicate the optimal sizing of each component within the system utilizing 1kW and 10 kW turbines. Given that the supply of renewable energy does not match the building's load demand and that the system operates off-grid, the significance of storage systems is greatly enhanced; consequently, the battery system constitutes the largest portion in terms of capacity. Specifically, the system incorporates 8,935 units of 1 kW lead-acid batteries. Additionally, a fuel cell with a capacity of 430 kW is designated as part of the storage system. The solar panels contribute over 1 MW of capacity to renewable energy generation. Moreover, the system utilizes 32 ten kW turbines, providing a total capacity of 320 kW from renewable energy sources.

Following the determination of the optimal size for each system component, their performance throughout the year is depicted in relation to the peak production levels illustrated in Fig. 10. The photovoltaic panels generate electricity during daylight hours, with peak production occurring between 11 AM and 3 PM, when sunlight intensity is at its highest (Fig. 10-a). These panels are capable of producing electricity for approximately 12 hours each day, though this duration decreases to around 9 hours during the winter months. Additionally, their output is diminished on cloudy or foggy days.

In contrast to solar energy, which is harnessed during specific daylight hours, wind turbines operate continuously throughout both day and night (Fig. 10-b). While solar panels experience reduced energy production in winter, wind energy can be harvested more effectively during this season. The differing peak production periods of wind and solar energy allow these sources to complement each other within a hybrid energy system, thereby enhancing the continuity of energy production.

Table 7. Optimized Sizing Results for 1 kW, 10kW Turbine.

Component	Name	Size		Unit
		1kW	10kW	
Generator	Fuel Cell CHP	430	430	kW
PV	Generic flat plate PV	1,202	1,137	kW
Storage	Generic 1kWh Lead Acid	9,535	8,935	strings
Wind turbine	Excel BWC XL.1kW--Bergey Excel – 10 kW	186	32	ea.
System converter	System Converter	417	417	kW
Boiler	Generic Boiler	1.00	1.00	quantity
Electrolyzer	Generic Electrolyzer	30.0	120	kW
Hydrogen tank	Hydrogen Tank	110	50.0	kg
Dispatch strategy	HOMER Load Following			

The fuel cell can ultimately provide an output power of 200 kW, with 159 starts and 159 operating hours annually, indicating limited operational frequency and duration throughout the day and year. Due to its infrequent use, the fuel cell has been categorized under disposal. When the solar panels, which have the highest production capacity, cease generating energy at sunset, the fuel cell begins to utilize stored hydrogen from the tank to produce electricity and heat. As shown in Fig. 10-c, the operational hours of the fuel cell typically coincide with sunset, a period during which the facility also demands a significant amount of energy, albeit less than during peak hours.

If wind energy and the fuel cell are insufficient to meet the building's load demand, the battery system is activated. As illustrated in Fig. 10-d, the battery system is more prominent during times when solar energy is available, indicating a higher state of charge. This condition is also maintained during periods when the wind turbine is operating at maximum output.

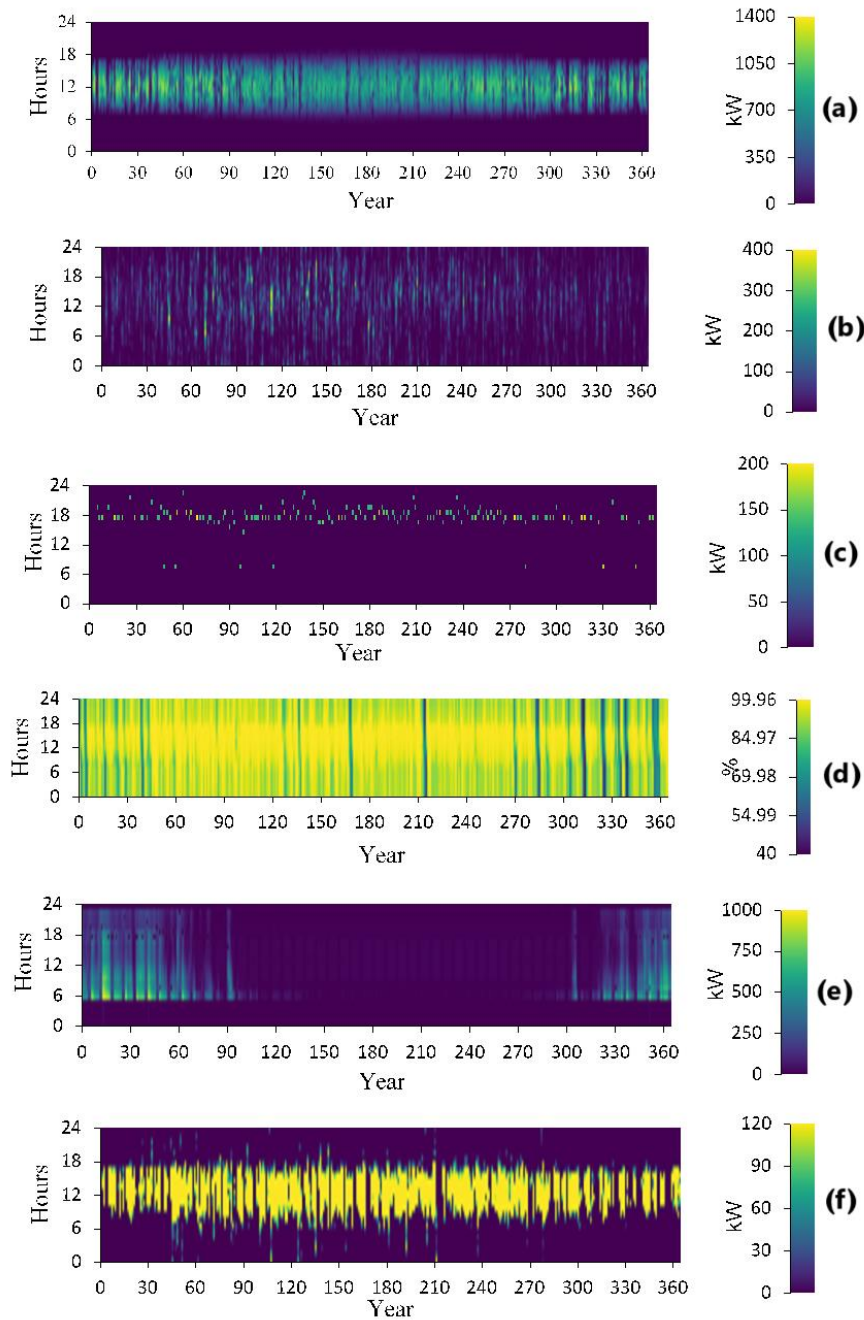


Fig. 10. (a) PV power output. (b) Wind turbine. (c) Fuel Cell. (d) Battery state of charge. (e) Boiler power output. (f) Electrolyzer input power.

Since the heat produced by the fuel cell does not fully satisfy the building's heating requirements, a boiler is employed for additional heat generation. As shown in Fig. 10-e, the boiler provides thermal energy output during the colder months, reaching a maximum output of 1,000 kW during the coldest hours of winter, which typically occur early in the morning. This peak output is clearly highlighted in the figure. During other nighttime and early morning hours when the facility is closed, boiler consumption is relatively low, dropping to zero from 11 PM to 5 AM.

During peak solar energy hours and periods of high wind speed, excess energy is directed to the electrolyzer to produce hydrogen for storage in the tank. As illustrated in Fig. 10-f, the electrolyzer operates at maximum output, generating nearly 120 kW of hydrogen during the hours when the output from both the solar panels and wind turbines is at its peak.

4.7. Technical Evaluation

4.7.1 Feasibility

For the system to be feasible, it must demonstrate both economic and technical viability. In the system utilizing 10 kW turbines, which provides more optimized conditions, the total current cost amounts to \$6.77 million, with an energy production cost of \$0.383 per kilowatt-hour. When compared to similar studies reviewed in the literature, it can be concluded that, considering the off-grid nature of the system and its reliance on renewable energy, as well as peak load conditions, this approach appears to be economically reasonable relative to other projects.

From a technical perspective, the photovoltaic system has a capacity that is three times greater than that of the wind turbine, while its electricity production is nearly nine times higher than that generated by wind energy. Consequently, wind energy is deemed inefficient for this location. The capacity of the solar panels is approximately 1.1 MW, while the wind system comprises 32 ten kW turbines. Establishing such a renewable energy facility necessitates a substantial area for both solar and wind farms.

The battery capacity is around 9,000 one-kilowatt batteries, which requires significant space for storage given the building's area. Considering the operational hours of the fuel cell, it only starts and operates for one hour on 159 days of the year, indicating insufficient utilization within the system. As a result, it will not be replaced throughout the project's lifespan, and its disposal costs are significantly offset. These factors suggest that the HOMER optimizer favors increased use of battery storage over hydrogen storage, indicating that hydrogen storage is not efficient under the given conditions.

4.7.2 Sensitivity Analysis

Following the initial assessment of system feasibility under current conditions, it was determined that the existing wind potential at the location is insufficient for the optimal utilization of wind turbines. To investigate the impact of increased wind speed on system performance, a sensitivity analysis was conducted by adding 2 meters per second to the average wind speed. This analysis allows for the evaluation of system performance under conditions akin to Tehran's climate but with enhanced wind potential.

The results of this analysis can inform the system's suitability for areas with similar climatic conditions but higher wind speeds. With the increase in wind speed, energy production from the wind turbine rose significantly, increasing from 10% to 64%, resulting in a generation of 1,772,017 kWh. In contrast, solar panel output decreased from 89% to 33.8%, producing 933,310 kWh (Table 8). This indicates that if the wind speed in Tehran were to increase by 2 meters per second, the potential for installing wind turbines would surpass that of solar panels, leading to a greater reliance on wind energy.

Furthermore, the production from fuel cells more than doubled, reinforcing the rationale for incorporating hydrogen storage into the system. Overall, total energy production increased due to the enhanced wind speed and the corresponding rise in wind energy generation.

Table 8. Total production after sensitivity analysis.

Component	Production (kWh/yr)	Percent
Generic flat plate PV	933,310	33.8
Fuel Cell CHP	57,922	2.10
Bergey Excel - S.60	1,772,017	64.1
Total	2,763,249	100

Table 9. Optimal size after sensitivity analysis.

Component	Name	Size	Unit
Generator	Fuel Cell CHP	430	kW
PV	Generic flat plate PV	549	kW
Storage	Generic 1kWh Lead Acid	3,817	strings
Wind turbine	Bergey Excel - S.60	102	ea.
System converter	System Converter	373	kW
Boiler	Generic Boiler	1.00	quantity
Electrolyzer	Generic Electrolyzer	250	kW
Hydrogen tank	Hydrogen Tank	270	kg
Dispatch strategy	HOMER Load Following		

With the increased reliance on hydrogen storage, the capacity of battery storage has been significantly reduced, decreasing from 8,935 one-kilowatt batteries to 3,817 units, representing a 57% reduction (as shown in Table 9). The capacity ratio of wind turbines to solar panels is 1.857, while the energy production ratio between them is 1.9. This indicates that, at equal capacities, wind turbines can generate slightly more energy than solar panels, demonstrating their greater efficiency.

The fuel cell maintains its capacity at 430 kilowatts, similar to previous configurations, but now produces more energy due to the increased overall system capacity resulting from higher hydrogen production. This enhancement in capacity for the electrolyzer and hydrogen tank facilitates greater utilization of hydrogen storage, although it necessitates additional physical space.

The current total cost of the system has decreased by 28%, bringing it to \$4.884 million, while the cost of energy production has also reduced by 28% to \$0.271 per kilowatt-hour. In this scenario, the wind turbine represents the largest share of costs at \$1.85 million, followed by the battery, which totals \$1.56 million, indicating that, with increased wind speed, battery costs have decreased by nearly 60%. The solar panel system has also experienced a significant reduction in total cost, now amounting to \$1.06 million, reflecting an approximate decrease of 51%. Furthermore, due to the increased utilization of the fuel cell, its disposal cost has been reduced to \$100,000, down from \$114,000 in the previous scenario (Fig. 11).

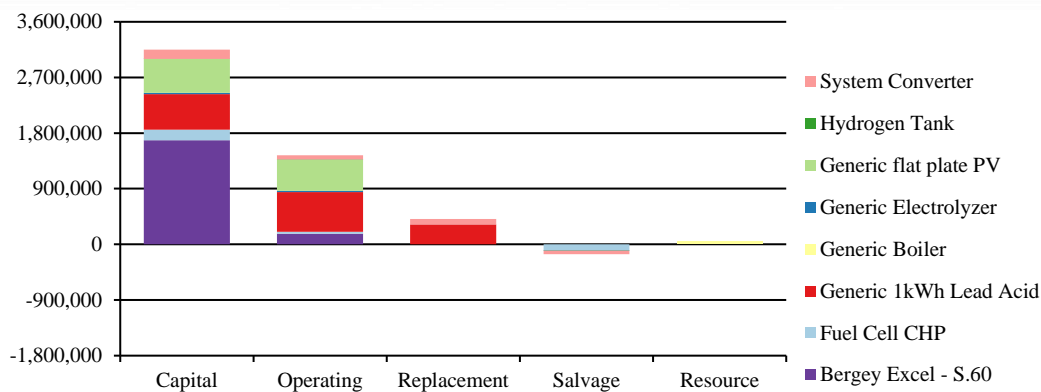


Fig 11. The economic details of the components after sensitivity analysis.

8. Conclusion

Addressing energy challenges in the building sector, a renewable energy system was implemented at one of the faculties of Amirkabir University as a case study for energy simulation. Given the intermittent nature of renewable energies, both hydrogen storage and batteries were integrated into the system. The feasibility of hydrogen storage and the effectiveness of wind energy utilization in Tehran were subsequently evaluated.

Two turbine capacities, 1 kW and 10 kW, were analyzed. The results indicated that in the 10 kW turbine system, solar energy produced 1,931,801 kWh (89%), wind energy generated 216,261 kWh (10%), and fuel cells contributed 1% of the total consumption. In the 1 kW turbine system, solar energy yielded 2,042,853 kWh (95%), while wind energy provided 112,852 kWh (5%), with negligible production from the fuel cells.

The total present cost for the 10 kW turbine system was \$6.77 million, with an electricity production cost of \$0.377 per kWh. For the 1 kW turbine system, the total present cost was \$6.87 million, and the electricity production cost was \$0.383 per kWh. In terms of CO₂ emissions, the 10 kW turbine system, benefiting from higher fuel cell production, reduced thermal energy generation from the boiler, resulting in an annual emission of 102,586 kg CO₂, compared to 103,787 kg CO₂ for the 1 kW turbine system.

The analysis indicated that the 10 kW turbine system is technically, economically, and environmentally superior, prompting a detailed output analysis for this configuration. A sensitivity analysis with increased wind speed revealed that wind energy production increased to 1,772,017 kWh (64% share), while solar panels generated 933,310 kWh (33.8% share) annually, substantiating the rationale for leveraging wind potential under these conditions. Additionally, fuel cell production more than doubled, enhancing the viability of hydrogen storage. The overall system became 28% more economically feasible.

Future work could involve developing a mathematical model for the system components to be utilized in a genetic algorithm (GA) or SAM software. The results of this model could be compared and evaluated using a multi-criteria decision-making (MCDM) algorithm to identify the optimal solution. Furthermore, the system could be designed and analyzed both with and without hydrogen storage and battery storage. The assessment may also include evaluating embedded carbon metrics to analyze environmental impacts and lifecycle considerations. This approach would facilitate a comprehensive evaluation of the sustainability of each storage solution, considering their operational efficiencies and associated carbon footprints throughout their respective lifecycles.

Declaration of competing interest

The authors declare that they have no known competing financial interests or personal relationships that could have appeared to influence the work reported in this paper.

Data availability

No data was used for the research described in the article.

References

- [1] Q. Wang, L. Duan, Z. Lu, N. Zheng, Thermodynamic performance comparison of SOFCMGT-CCHP systems coupled with two different solar methane steam reforming processes, *International Journal of Hydrogen Energy*, 48 (2023) 71: 27473-27491.
- [2] S. Lu, Y. Li, H. Xia, Study on the configuration and operation optimization of CCHP coupling multiple energy system, *Energy Conversion and Management*, 177 (2018): 773-791. <https://doi.org/10.1016/j.enconman.2018.10.006>.
- [3] I.B. Mansir, E.H. Bani Hani, N. Farouk, A. AlArjani, H. Ayed, D. Duc Nguyen, Comparative transient simulation of a renewable energy system with hydrogen and battery energy storage for residential applications, *International Journal of Hydrogen Energy*, 47 (2022) 62: 26198-26208.
- [4] J. Zhou, Y. Wu, H. Dong, Y. Tao, C. Xu, Proposal and comprehensive analysis of gas-wind-photovoltaic-hydrogen integrated energy system considering multi-participant interest preference, *Journal of Cleaner Production*, 265 (2020).
- [5] I.B. Mansir, E.H. Bani Hani, H. Ayed, C. Diyoke, Dynamic simulation of hydrogen-based zero energy buildings with hydrogen energy storage for various climate conditions, *International Journal of Hydrogen Energy*, 47 (2021) 62: 26501-26514.
- [6] A.A.M. Aljabery, H. Mehrjerdi, S. Mahdavi, R. Hemmati, Multi carrier energy systems and energy hubs: Comprehensive review, survey and recommendations, *International Journal of Hydrogen Energy*, 46 (2021) 23795-23814.
- [7] Y. Noorollahi, H. Yousefi, R. Moltames, R. Fattahi, Performance evaluation of hydrogen production system using CPVT/ROC, *Journal of Renewable and New Energy*, 10 (2023) 36-45.
- [8] Z. Lu, L. Duan, Z. Wang, Performance evaluation of a novel CCHP system integrated with MCFC, ISCC, and LiBr refrigeration system, *International Journal of Hydrogen Energy*, 47 (2022).
- [9] R.-G. Wang, Y.-I. Guo, K.-X. Liu, J.-S. Wang, L.-S. Dai, Performance analysis of building hydrogen comprehensive utilization system based on CCHP system of hydrogen fuel cell, 2nd IEEE Conference on Energy Internet and Energy System Integration (EI2), Beijing, China, 2018, pp. 1-6.
- [10] M. Li, K. Zhu, Y. Lu, Q. Zhao, K. Yin, Technical and economic analysis of multi-energy complementary systems for net-zero energy consumption combining wind, solar, hydrogen, geothermal, and storage energy, *Energy Conversion and Management*, 295 (2023).
- [11] F. Homayouni, R. Roshandel, A.A. Hamidi, Techno-economic and environmental analysis of an integrated standalone hybrid solar hydrogen system to supply CCHP loads of a greenhouse in Iran, *International Journal of Green Energy*, 14 (2016) 3.
- [12] A.K. Sleiti, W.A. Al-Ammari, R. Arshad, Energetic, economic, and environmental analysis of solid oxide fuel cell-based combined cooling, heating, and power system for cancer care hospital, *Building Simulation*, 15 (2022) 1437-1454.
- [13] J. Zhao, H. Chang, X. Luo, Z. Tu, S.H. Chan, A novel type of PEMFC-based CCHP system with independent control of refrigeration and dehumidification, *Applied Thermal Engineering*, 204 (2022).
- [14] Q. Hou, H. Zhao, X. Yang, Economic Performance Study of the Integrated MR-SOFC-CCHP System, *Energy*, 166 (2019) 236-245.
- [15] N. Li, X. Zhao, X. Shi, Z. Pei, H. Mu, F. Taghizadeh-Hesary, Integrated energy systems with CCHP and hydrogen supply: A new outlet for curtailed wind power, *Applied Energy*, 303 (2021).
- [16] F. Bahramian, A. Akbari, M.R. Nabavi, S. Esfandi, E. Naeiji, A. Issakhov, Design and tri-objective optimization of an energy plant integrated with near-zero energy building including energy storage: An application of dynamic simulation, *Sustainable Energy Technologies and Assessments*, 47 (2021) 101419.
- [17] Y. Song, H. Mu, N. Li, X. Shi, X. Zhao, C. Chen, H. Wang, Techno-economic analysis of a hybrid energy system for CCHP and hydrogen production based on solar energy, *International Journal of Hydrogen Energy*, 47 (2022) 57.
- [18] E.B. Agyekum, J.D. Ampah, S. Afrane, T.S. Adebayo, E. Agbozo, A 3E, hydrogen production, irrigation, and employment potential assessment of a hybrid energy system for tropical weather conditions: Combination of HOMER software, Shannon entropy, and TOPSIS, *International Journal of Hydrogen Energy*, 47 (2022).
- [19] D.N. Luta, A.K. Raji, Decision-making between a grid extension and a rural renewable off-grid system with hydrogen generation, *International Journal of Hydrogen Energy*, 43 (2018) 20: 9535-9548.
- [20] B. Modu, M.P. Abdullah, A.L. Bakar, M.F. Hamza, M.S. Adewolu, Energy management and capacity planning of photovoltaic-wind-biomass energy system considering hydrogen-battery storage, *Energy Storage*, 73 (2023).
- [21] M.H. Jahangir, S. Fakouriyani, M. Amin, V. Rad, Feasibility study of on/off grid large-scale PV/WT/WEC hybrid energy system in coastal cities: A case-based research, *Renewable Energy*, 162 (2020) 2075-2095.
- [22] A.L. Bakar, et al., Energy management strategy and capacity planning of an autonomous microgrid: performance comparison of metaheuristic optimization searching techniques, *Renewable Energy Focus*, 40 (2022) 48-66.
- [23] J. Zhou, Z. Xu, Optimal sizing design and integrated cost-benefit assessment of stand-alone microgrid system with different energy storage employing chameleon swarm algorithm: a rural case in Northeast China, *Renewable Energy*, 202 (2023) 1110-1137.
- [24] K. O. S. Suhag, Techno-economic analysis of a hybrid renewable energy system for an energy poor rural community, *Journal of Energy Storage*, 23 (2019).
- [25] O. L., S. Mekhilef, A.S.N. Huda, K. Sanusi, Techno-economic analysis of hybrid PV-diesel-battery and PV-wind-diesel-battery power systems for mobile BTS: the way forward for rural development, *Energy Science & Engineering*, 3 (2015).
- [26] X. Xu, W. Hu, Di Cao, Qi Huang, W. Liu, M.Z. Jacobson, et al., Optimal operational strategy for an off-grid hybrid hydrogen/electricity refueling station powered by solar photovoltaics, *Journal of Power Sources*, 451 (2020) 227810.

- [27] A. Ursúa, E.L. Barrios, J. Pascual, I. San Martín, P. Sanchis, Integration of commercial alkaline water electrolyzers with renewable energies: limitations and improvements, *International Journal of Hydrogen Energy*, 41 (2016) 12852–61.
- [28] A. Maleki, Design and optimization of autonomous solar-wind-reverse osmosis desalination systems coupling battery and hydrogen energy storage by an improved bee algorithm, *Desalination*, 435 (2018).
- [29] S. Pelaez-Pelaez, A. Colmenar-Santos, C. Perez-Molina, A.-E. Rosales, E. Rosales-Asensio, Techno-economic analysis of a heat and power combination system based on hybrid photovoltaic-fuel cell systems using hydrogen as an energy vector, *Energy*, 224 (2021).
- [30] M. Thirunavukkarasu, Y. Sawle, An examination of the techno-economic viability of hybrid grid-integrated and stand-alone generation systems for an Indian tea plant, *Frontiers in Energy Research*, 10 (2022).
- [31] V. MZ, M. Hajivand, M. Moshkelgosha, N. Parsa, H. Mansoori, Optimal, reliable and economic designing of renewable energy photovoltaic/wind system considering different storage technology using intelligent improved slap swarm optimization algorithm: commercial application for Iran, *International Journal of Sustainable Energy*, 39 (2020) 5.
- [32] L. El boujdaini, F. Jurado, A. Mezrhab, M.A. Moussaoui, D. Vera, Cost and size optimization of hybrid solar and hydrogen subsystem using HOMER Pro software, *International Journal of Hydrogen Energy*, 48 (2023) 62: 24018-24036.
- [33] HOMER Help Manual, 2015.
- [34] H. Yazdani, M. Baneshi, M. Yaghoubi, Techno-economic and environmental design of hybrid energy systems using multi-objective optimization and multi-criteria decision making methods, *Energy Conversion and Management*, 282 (2023).
- [35] M.H. Ghodusinejad, Z. Lavasani, H. Yousef, A combined decision-making framework for techno-environmental-economic assessment of a commercial CCHP system, *Energy*, 276 (2023).
- [36] A. Toopshekan, P. Rahdan, M.A. Vaziri Rad, H. Yousefi, F. Razi Astaraci, Evaluation of a stand-alone CHP-Hybrid system using a multi-criteria decision making approach due to the sustainable development goals, *Sustainable Cities and Society*, 87 (2022).
- [37] K.E. Okedu, R. Uhumwangho, Optimization of renewable energy efficiency using HOMER, *International Journal of Renewable Energy Research (IJRER)*, 4 (2014): 421-427.
- [38] T.R. Ayodele, T.C. Mosele, A.A. Yusuff, A.S.O. Ogunjuyigbe, Off-grid hybrid renewable energy system with hydrogen storage for South African rural community health clinic, *International Journal of Hydrogen Energy*, 46 (2021) 38.
- [39] E. Kalamaras, M. Belekoukia, Z. Lin, B. Xue, H. Wang, J. Xuan, Techno-economic assessment of a hybrid off-grid DC system for combined heat and power generation in remote islands, *Energy Procedia*, 158 (2019).
- [40] M. Jahangiri, F. Karimi Shahmarvandi, R. Alayi, Renewable energy-based systems on a residential scale in southern coastal areas of Iran: Trigeneration of heat, power, and hydrogen, *Journal of Renewable Energy and Environment*, 8 (2021) 4: 67-76.
- [41] H. Kim, B. Seo, P. Eunil, J. Hyun Ch., Optimal green energy management in Jeju, South Korea – On-grid and off-grid electrification, *Renewable Energy*, 69 (2014): 123–133.